

Renewable Polymers from Passion Fruit Vegetable Oils Extracted by Different Methods

Polímeros Renováveis obtidos a Partir de Óleos Vegetais de Maracujá Extraídos por Diferentes Métodos

Victória R. A. Carneiro,^a Caroline Gaglieri,^a Rafael T. Alarcon,^b Gabriel I. Santos,^a Fernanda B. Santos,^a Gilbert Bannach^{a,*}

^a Universidade Estadual Paulista (UNESP), Faculdade de Ciências, Departamento de Química, CEP 17033-260, Bauru-SP, Brasil

^b Universidade de São Paulo, Instituto de Química de São Carlos, CEP 13566-590, São Carlos-SP, Brasil

*E-mail: gilbert.bannach@unesp.br

Recebido: 26 de Outubro de 2023

Aceito: 17 de Abril de 2024

Publicado online: 24 de Abril de 2024

The vegetable oil extraction process can interfere with the characteristics of the final product, including color and unsaturated quantity. However, no study has analyzed this effect in vegetable oil-based polymeric materials. Therefore, this work evaluates two different extraction methods for passion fruit vegetable oil and their influence on polymeric materials, comparing the results with one polymer obtained by commercial vegetable oil. The polymers syntheses were performed in the absence of solvent nor catalyst and performed by conventional heating. Properties as iodine values and fatty acid profile did not vary significantly among the oils. However, color and thermal stability varied between the vegetable oils, especially due to the presence of small molecules that can be extracted during the Soxhlet process. As a result, the final polymers also presented different colors. For this type of polymerization, the extraction processes did not interfere significantly in thermal stability, glass transition, spectroscopic data nor morphological properties of final polymers.

Keywords: Passion fruit vegetable; renewable polymers; glycerol.

1. Introduction

Polymers from fossil resources have become a problem, due to their slow degradation, causing environmental issues. Therefore, scientific research is focused on developing new renewable polymers from renewable sources.^{1,2} Renewable polymers are sustainable and can provide better environmental preservation than petroleum-based polymers.²

Vegetable oils are renewable sources^{3,4} and can be modified by epoxidation, maleinization, acrylation, and carbonation reactions to provide renewable monomers.⁵⁻⁷ The modification procedure occurs in the alkene group (unsaturation) presented in the fatty acid chain. Each vegetable oil has three fatty acid chains linked by a glyceride backbone.^{8,9}

Different fruit sources provide vegetable oil with different levels of unsaturation. Passion fruit provides a vegetable oil with 86% of unsaturation, which consists of linoleic acid (66.3%), oleic acid (18.7%), and linolenic acid (0.3%). In addition, these values can be affected by the extraction method.^{10,11}

Passion fruit is from the America tropics and is usually used in juice manufacture. Its peel and seed are discarded in the juicing process, resulting in a waste of 52%.¹²⁻¹⁴ Passion fruit vegetable oil (PFVO) is extracted directly from its seeds using a solvent, cold-pressing, hot-pressing, and other methods. Because the extraction type can interfere with the yield, oil quality, and fatty acid profile, the quantity of antioxidants and carotenoids depends on the extraction type.¹⁵

Polymers based on vegetable oil have broad applications in industry. Polymers from renewable sources have been used as biosensors, encapsulating agents, and adsorbents.³ Furthermore, vegetable oils have been used as photosensitive monomers to produce polymeric materials in 3D printers and have increased their application.¹⁰

Although it is known that the extraction procedure can interfere with the color and Iodine Value (IV), the literature does include studies about the effect of these procedures on the final properties of a renewable polymer derived from vegetable oils or in the thermal behavior of the vegetable oils. Thus, the present work evaluated how PFVO obtained from different extractions can interfere with these physical-chemical properties.

2. Experimental Section

2.1. Chemicals

The reactants maleic anhydride (MA, Sigma-Aldrich, >99%), glycerol (Sigma Aldrich, 99.5%), and ethyl acetate (LabSynth, 99.3%) were received and used in this work without further purification. The first vegetable oil (PFVO1) was purchased from Mundo dos Óleos® (Brasília, Brazil), which also extracts the vegetable oil from seeds using cold pressing in a more controlled manner.¹⁶ The other vegetable oils (PFVO2 and PFVO3) were extracted from fruits purchased at a local market.

2.2. Extraction procedures

First, the seeds from passion fruit (*Passiflora edilis*) were extracted, washed, and dried at 80 °C for 12 h. They were then stored in a dried and cleaned plastic vessel. The vegetable oil was extracted using two different processes (hot-pressing and Soxhlet solvent extraction).

Seeds were placed in hot-pressing equipment (model Yoda MQO 001, Home up), which was heated to 70 °C to release the vegetable oil (PFVO2). The other seeds were added into the Soxhlet system. Although literature reports that hexane extracts vegetable oil in a greater quantity than acetone or isopropyl alcohol,¹⁷ it was used ethyl acetate because it is considered a green solvent (safer and sustainable).¹⁸ The Soxhlet system was refluxed for 3 h; then, the extract was put in a rotary evaporator to evaporate the ethyl acetate (60 °C and 400 mmHg), obtaining the passion fruit vegetable oil (PFVO3).

2.3. Synthesis of pre-polymer (PP)

The PP was synthesized using a molar proportion of maleic anhydride: glycerol equal to 3:2. First, in a beaker, the maleic anhydride and glycerol were heated up to 60 °C (near to its melting temperature)¹⁹ and kept at this temperature until its completed melting. Then, the system was heated up to 120 °C and kept stirring to obtain a viscous, yellowish liquid.

2.4. Synthesis of renewable polymers

After the PP synthesis, it was heated to 120 °C, and the vegetable oil was added (30 wt% of PP). The temperature was increased to 230 °C, kept for 10 minutes, and then heated up to 300 °C. After a few minutes, the solid polymers (PPFs) were obtained. The three different PFVOs resulted in different PPFs: the PFVO1 resulted in the PPF1, PFVO2 in the PPF2, and PFVO3 in the PPF3.

2.5. Characterization

2.5.1. Iodine value (IV)

The iodine value (IV) measures the average of double bonds present in the vegetable oil sample, and it is defined as the gram of halogen (iodine) adsorbed by 100 g of sample (expressed as gram of I₂).¹⁰ The IV procedure was obtained by titration method following the AOCS 3d-63 method.²⁰ In addition, it was determined by ¹H-NMR, following the procedure previously described.⁵

2.5.2. Mid-Infrared Spectroscopy (MIR)

The spectra in the infrared region of the samples were obtained using a Vertex 70 spectrometer (Bruker) through the attenuated total reflectance method with a scanning range between 600 and 4000 cm⁻¹ (resolution of 4 cm⁻¹) using diamond crystal as support.

2.5.3. ¹H-NMR analyses

The ¹H-NMR (nuclear magnetic resonance) analyses were performed to compare the structure of vegetable oil obtained from each extraction method. Ascend III 600 MHz spectrometer was employed for the ¹H-NMR spectra using tetramethylsilane (TMS) as an internal reference. All samples (5 mg) were solubilized in deuterated chloroform (CDCl₃). The polymers were not analyzed due to their insolubility in the usual deuterated solvents. The profile of fatty acid chains was determined following the procedure in the literature.²¹

2.5.4. Ultra-Violet and Visible Light Spectroscopy (UV-Vis)

The Ultra-Violet and Visible Light absorption spectra (UV-Vis) of vegetable oils were obtained in a SpectraMax M2 spectrophotometer (Molecular Devices) using a 1.0 cm light path quartz cuvette at room temperature and ethyl acetate as solvent.

2.5.5. Simultaneous Thermogravimetry-Differential Thermal Analysis (TG-DTA) and Differential Scanning Calorimetry (DSC)

TG-DTA curves were obtained using the thermal analysis system from Netzsch, model STA 449 F3. The samples were placed in a 200-μL α-alumina open crucible, the other parameter were set as heating rate of 10.0 °C min⁻¹ and a flow rate of 70 mL min⁻¹ in a dry air atmosphere. The temperature range and sample mass used for the vegetable oils and their respective polymers were 30.0–800.0 °C, and 27 mg, respectively.

For the DSC analyses, a Mettler-Toledo DSC1 Star[®] system was employed, using approximately 10 mg of sample, which was placed in a closed aluminum crucible with a perforated lid. The equipment was set at a heating rate of 10 °C min⁻¹ using a dry air atmosphere with a flow rate of 50 mL min⁻¹. The heating/cooling procedures were performed in the range of -35–120 °C (for vegetable oils) and until 230 °C (polymers).

2.5.6. Scanning Electron Microscopy (SEM)

An EVO LS15 scanning electronic microscope from Zeiss was used to study the morphology of each polymer. The samples were prepared by powdering them, placing them over a carbon adhesive, and finally plating them with gold. The voltage was set at 15 kV, and the samples were magnified 1000 times in a high vacuum environment (10^{-3} Pa).

3. Results and Discussion

The commercial vegetable oil (PFVO1) and the extracted passion fruit vegetable oils: PFVO2 (extracted by hot-pressing) and PFVO3 (extracted by Soxhlet) can be seen in Figure 1a. Each passion fruit vegetable oil has a different color (colorless, dark yellow, and dark orange). The PFVO3 has the darkest color, exhibiting small particles in the suspension, which can be attributed to solid terpenes (soluble in ethyl acetate). In addition, the PFVO3 has a fruity aroma, unlike the other samples. The different colors can be attributed to the small components of each oil, which can vary according to the extraction method and the ambient conditions in which the plant had been raised.⁹ Hence, the synthesized polymers (Figure 1-b) also have different colors. The PPF1 and PPF2 exhibited a light-yellowish color, while PPF3 had a shiny brown color and a slight fruity aroma.

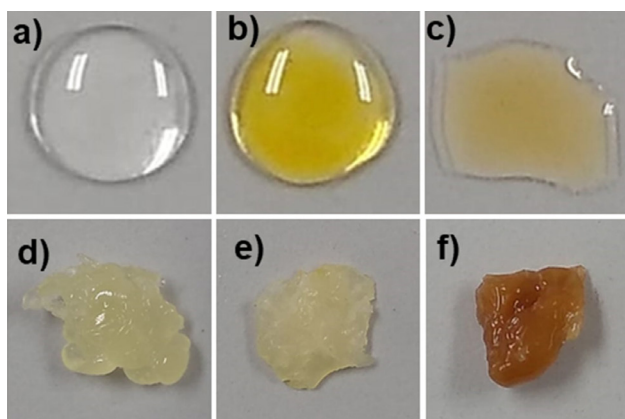


Figure 1. Passion fruit vegetable oil images: a) PFVO1, b) PFVO2, and c) PFVO3, as well as their respective polymers: d) PPF1, e) PPF2, and f) PPF3

3.1. Iodine value (IV)

The values (in grams of I_2 per 100 g of sample) obtained by titration for PFVO1, PFVO2, and PFVO3 were 123.1 ± 1.1 ; 126.0 ± 0.9 ; and 121.5 ± 1.2 , respectively. Although the extraction methods and color differ, all samples can be considered semi-drying oils.¹⁰ They are similar to grape seed oil (121.58 ± 0.86 g I_2 per 100 g of sample) and soybean oil (126.32 ± 2.08 g I_2 per 100 g of sample).^{6,7}

3.2. MIR

Figure 2 exhibits the MIR spectra of PP, PFVO, and PPF1 samples. The three most important bands in this work are outlined in the figure. A wide band between 3670 - 3150 cm^{-1} in the spectrum of PP (Figure 2a), is resulting from O-H stretching (highlighted in green). This band is also present in the polymer spectrum (Figure 2c). In addition, the PP (Figure 2a) does not contain residual maleic anhydride, indicated by the absence of the bands at 1776 and 1853 cm^{-1} in the PP spectrum.¹⁹ In addition, the band at 1643 cm^{-1} in the PP spectrum is associated with C=C stretching from the maleic anhydride derivative ester. In the PFVO1 spectrum (Figure 2b), the band resulting from this stretching appears as a small one at 1654 cm^{-1} (indicated by a red arrow), while in the PPF1 spectrum (Figure 2c), this band is observed at 1645 cm^{-1} . The intense bands centered at 3008 , 2923 and 2854 cm^{-1} in PFVO1 spectra (Figure 2b) are resulting from the different C-H stretching in the chain, in which the first one refers to stretching of vinyl hydrogen from C=C-H, the second band refers to methyl groups and the last one is resulting from methylene groups.⁶ These bands are also present in PPF1 spectrum (Figure 2c); however, they present small intensity, since the fraction of vegetable oil in the system is only 30 wt%.

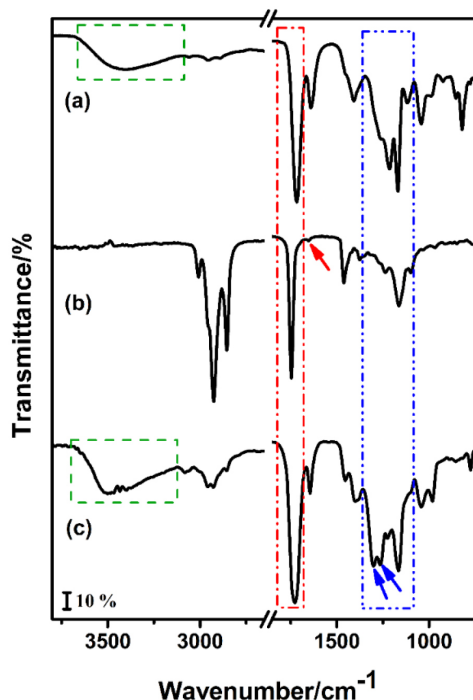


Figure 2. MIR spectra of precursors a) PP, b) PFVO1, and c) the polymer PPF1

All spectra display the band of C=O stretching (highlighted in red) resulting from carbonyl ester. In the PP sample (Figure 2a), it appears at 1716 cm^{-1} , and its displacement to lower wavenumber values can be associated with the presence of α,β unsaturated conjugation in the PP.²²

The intense band at 1747 cm^{-1} (Figure 2b) is from C=O stretching present in the triglycerides chain. In the PPF1 polymer, the carbonyl band is large at 1728 cm^{-1} and can be assigned to the overlapping of the carbonyl esters from PP and PFVO1 chains.^{22,23}

Moreover, the region highlighted in blue is characteristic of C-O stretching. Although bands are common in all samples, in the PPF1 spectrum (Figure 2c), two new bands are observed at 1263 cm^{-1} and 1302 cm^{-1} (indicated by blue arrows). These bands indicate the presence of new esters, different from those observed in PP and VO samples. Due to the similarity between the MIR spectra, the respective spectra are shown in Figure S1.

3.3. $^1\text{H-NMR}$ of vegetable oils

Figures 3a to 3c display the main regions of $^1\text{H-NMR}$ spectra of the PFVO samples. The complete spectra can be seen in Figure S2 (in Supplementary Material). They all present the same signals without significant changes. The signal at 0.98 ppm (magnified in Figure 3) is a characteristic triplet resulting from the methyl hydrogens of the linoleate chain. As a result, they present a small amount of this fatty ester (Table 1). Although the values of the saturated

chains are close to 18% in all samples, the number of polyunsaturated chains is higher in the PFVO2 and PFVO3 samples. The linoleic chain is the most abundant in all samples of passion fruit vegetable oil, which is in accordance with other works in the literature.²⁴⁻²⁶ In addition, the IV values calculated by $^1\text{H-NMR}$ (Table 1) are very similar to those obtained by titration, corroborating that all samples are considered semi-drying oil.

3.4. UV-Vis

Ultra-violet and visible light spectroscopy analyses (UV-Vis) were performed to verify why each sample has a different color. Spectra of the samples can be seen in Figure 4.

The most intense band in all spectra refers to the allowed transition $\pi\rightarrow\pi^*$ attributed to carbonyl groups (C=O) from the triglycerides. Usually, this band occurs around 190 nm in simple carbonyl compounds. However, a bathochromic displacement leads to longer wavelengths due to unsaturated bonds from the fatty acid chains. In the PFVO1 spectrum, the band associated with the $\pi\rightarrow\pi^*$ transition from the carbonyl groups appears at 252 nm. In the spectra of PFVO2 and PFVO3, the $\pi\rightarrow\pi^*$ transition from the carbonyl groups

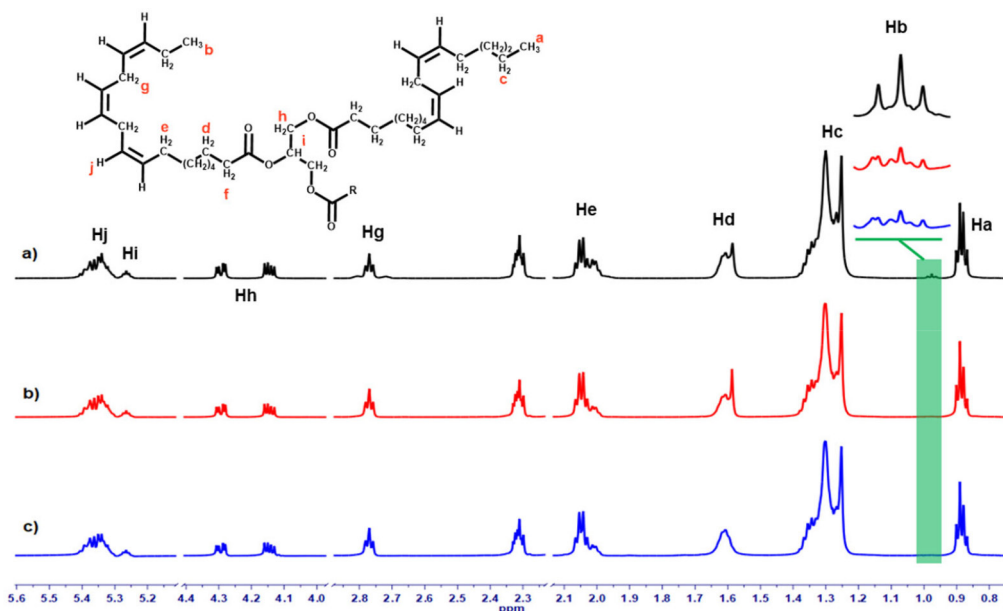


Figure 3. $^1\text{H-NMR}$ spectra (600 MHz, CDCl_3) of different passion fruit vegetable oils: a) PFVO1, b) PFVO2, and c) PFVO3, representative structure of a triglyceride and its respective protons

Table 1. IV and percentage of unsaturated and saturated chains obtained by $^1\text{H-NMR}$ for each passion fruit vegetable oil.

	IV by $^1\text{H-NMR}$	Oleic (%)	Linoleic (%)	Linolenic (%)	Total of monounsaturated (%)	Total of polyunsaturated (%)	Total of saturated (%)
PFVO1	119.4	30.1	48.1	4.4	30.1	52.5	17.4
PFVO2	128.2	20.6	59.3	2.1	20.6	61.4	18.0
PFVO3	121.5	22.2	55.7	3.3	22.2	59.0	18.8
PFVO3- heated until $240\text{ }^\circ\text{C}$	122.4	23.2	54.5	3.1	23.2	57.6	19.2

exhibits a bathochromic displacement compared to the previous samples, which is evidenced at 290 nm and 288 nm, respectively.

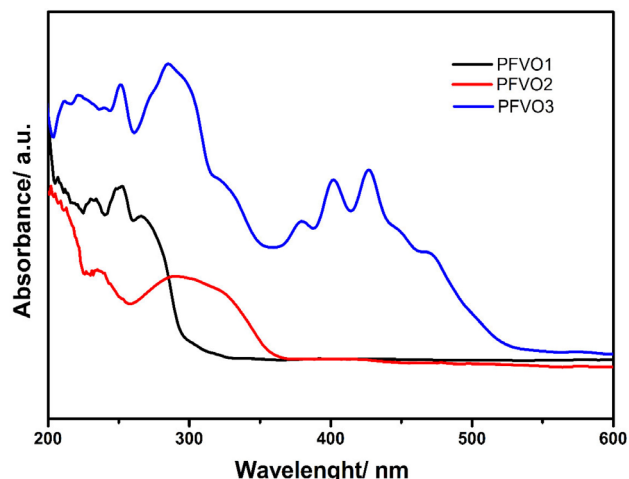


Figure 4. UV-Vis spectra of different passion fruit vegetable oils: PFVO1, PFVO2, and PFVO3

A minor intensity band can be observed in all samples next to the $\pi \rightarrow \pi^*$ transition band at larger wavelengths, corresponding to the prohibited $n \rightarrow \pi^*$ transition of the carbonyl groups. This band does not evidence a pronounced bathochromic displacement similar to the $\pi \rightarrow \pi^*$ transition band due to increased unsaturated bonds. In the PFVO2 and PFVO3 spectra, this band appears at 325 nm.

The PFVO2 and PFVO3 samples present larger bathochromic displacement than PFVO1 in both $\pi \rightarrow \pi^*$ and $n \rightarrow \pi^*$ transitions from the carbonyl group. Furthermore, the PFVO3 sample presents other $n \rightarrow \pi^*$ transitions on the visible region related to the conjugation between unsaturated bonds (C=C) and the carbonyl group (C=O), which explains the brownish color in the sample. This may be associated with the presence of small molecules in the sample, which were also extracted by Soxhlet (their presence will be better discussed in the next section). Bands with a wavelength less than 250 nm are related to the $\pi \rightarrow \pi^*$ transitions from the unsaturated bond between carbons (C=C).

3.5. TG/DTG-DTA curves

The TG/DTG-DTA curves for PFVO1, PFVO2 and PFVO3 are presented in Figure 5, while the respective polymers are shown in Figure 6. In addition, the information related to each step of mass loss is provided in Table S1.

All the vegetable oil samples have a similar TG curve profile except for PFVO3 (Figure 5c). The other two PFVO samples are stable up to 270.0 °C, with two steps of mass losses associated with exothermic peaks in the DTA curve (Table S1). The TG curve for PFVO3 (Figure 5c) shows a small and continuous step of mass loss from 68.8 to 240.0 °C ($\Delta m = 4.97\%$) that may be attributed to degradation/evaporation of volatile compounds in vegetable

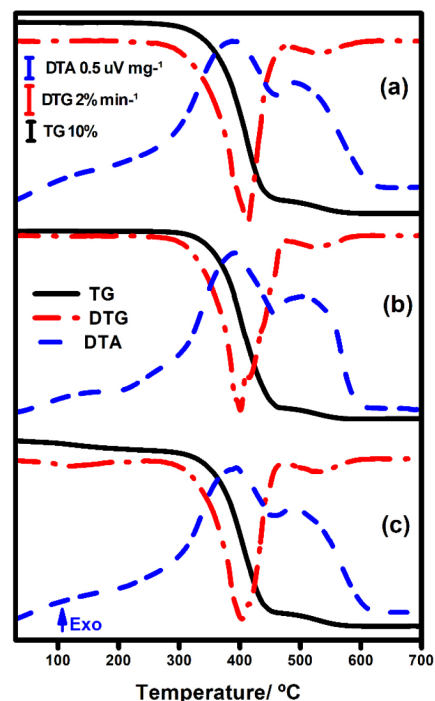


Figure 5. TG/DTG-DTA curves of different passion fruit vegetable oils: a) PFVO1, b) PFVO2, and c) PFVO3

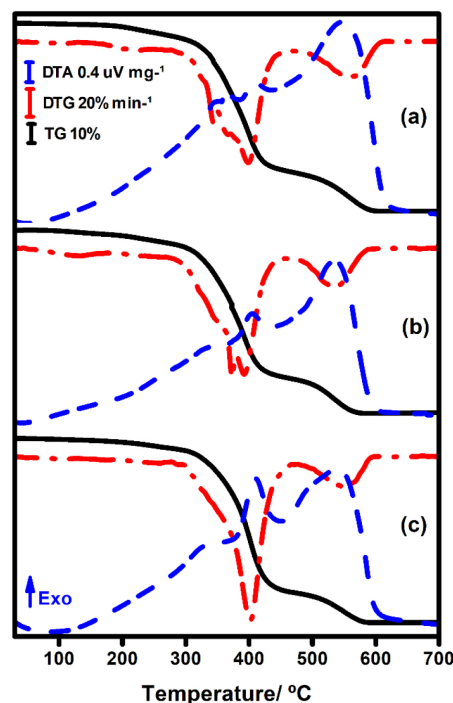


Figure 6. TG/DTG-DTA curves of polymers obtained from different passion fruit vegetable oils: a) PPVO1, b) PPVO2, and c) PPVO3

oil from passion fruit.²⁵ This mass loss, which will be better discussed in the DSC section, cannot be attributed to residual ethyl acetate due to the absence of the signal at 2.05 ppm (Figure S2c) from ethyl acetate as a contaminant in deuterated chloroform.²⁷ In addition, the IV value did not change after this mass loss, which indicates that it is not

the degradation of the triglyceride chain of PFVO3. These chains start the degradation process at 287.6 °C, and two steps of mass loss are observed in the TG curve related to vegetable oil degradation and associated with exothermic peaks in the DTA curve. Table 1 shows the detailed thermal events. Despite the similarity of TG curves, the DTG curves are different. While the PFVO2 exhibited two overlapping and consecutive steps in DTG (resulting in one mass loss in the TG curve), the samples PFVO1 and PFVO3 have one broad peak in the DTG curve. These results suggest that the thermal decomposition of PFVO is not the same, which could be attributed to small changes in their composition.

The polymers (Figure 6) also have a similar TG curve profile: a small and continuous mass loss before their thermal stability associated with the water evaporation, which can be present on the surface or in cages (from the condensation reaction in the polymerization process). Then, two steps of mass loss associated with exothermic peaks are observed in TG-DTA curves. The shape and intensity of the exothermic peaks in DTA curves differ for each sample. For example, three exothermic peaks (with similar intensity) are observed in the DTA curve of PPF1 (Figure 6a) related to the second mass loss and are less intense than the exothermic peak observed for the third mass loss. However, for the PFOV2 (Figure 6b), all exothermic peaks show similar intensity. The DTA curves indicate changes in the thermal decomposition of polymers. This is supported by the changes in the maximum degradation rate for each polymer.

3.6. DSC curves

The cyclic DSC curves of PFVO1 and PFVO2 are present in Figures 7a and 7b, respectively. They exhibited a similar behavior: an exothermic event related to the crystallization process in the cooling and an endothermic event associated with the melting process in the heating. The temperature peaks and enthalpy do not change significantly between these samples (Table S2).

The DSC curve of PFVO3 is exhibited in Figure 7c. The temperature range used for it was higher to study the mass loss observed in its TG curve (Figure 5c), which was absent in the other passion fruit vegetable oils. It also presents the crystallization and melting processes during the first cooling and first heating, respectively. However, after the melting of the sample, an endothermic event was observed ($T_p = 174.5$ °C and $\Delta H = 47.0$ J g⁻¹), which may be attributed to the evaporation of volatile compounds that can be found in passion fruit vegetable oil.²⁵ The sample was heated to 240 °C, and then a MIR and ¹H NMR were collected (Figures S3 and S4, respectively). The samples present similar profiles in both analyses. However, a small change is observed in the region between 1250-1000 cm⁻¹ by MIR (magnified in Figure S3), especially the absence of the band at 1047 cm⁻¹ (red arrow) and modification of the one at 1238 cm⁻¹ (blue arrow) after the heating. Small changes are also observed in ¹H NMR spectra,

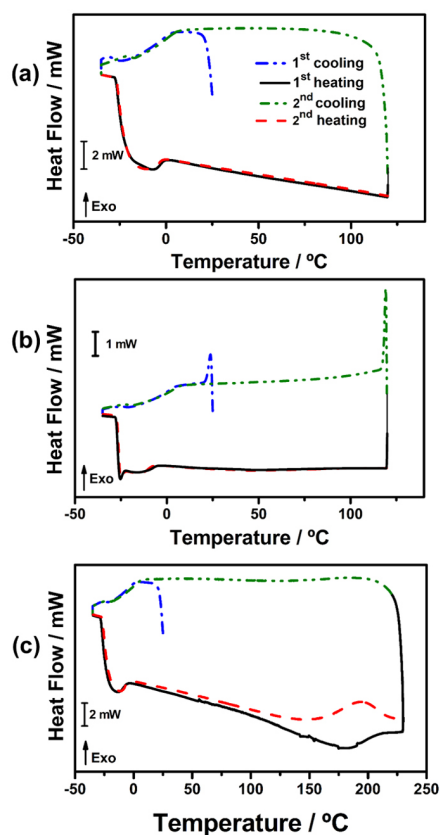


Figure 7. DSC curves of a) PFVO1, b) PFVO2, and c) PFVO3

and they are magnified in Figure S4. Most small signals from 3.80-3.50 and 2.00-1.70 ppm disappeared after the sample heating. In addition, the IV value obtained by ¹H NMR was equal to 122.4, and the fatty acid profile is very similar to that obtained before the heating (Table 1). These results corroborate the presence of small volatile molecules in PFVO3, which were extracted together with the triglyceride in the extraction process and resulted in the small mass loss in the TG curve (Figure 5c, Table S1) and the endothermic event observed in the first heating in DSC curve (Figure 7c). These volatile compounds could be esters, ketones, aldehydes, and terpenes and result in the aromatic properties of oil.²⁵ Consequently, the crystallization and melting enthalpy decrease in the second stage. Moreover, the crystallization and melting processes dislocate to higher temperatures (Table S2) and are observed an exothermic peak during the second heating ($T_p = 194.2$ °C and $\Delta H = 22.3$ J g⁻¹), which may be attributed to the degradation of less volatile compounds (confirmed by observation of small particles suspended in the PFVO3 after opening the crucible at the end of analysis).

The DSC curves obtained for the polymers PPF are shown in Figure 8. All samples had a broad endotherm event in the first heating associated with the water evaporation (from surface and cages), observed in the first mass loss in the TG curve for each polymer. In addition, all samples presented a glass transition in the cooling stage and were more visible in the second heating. Although the onset

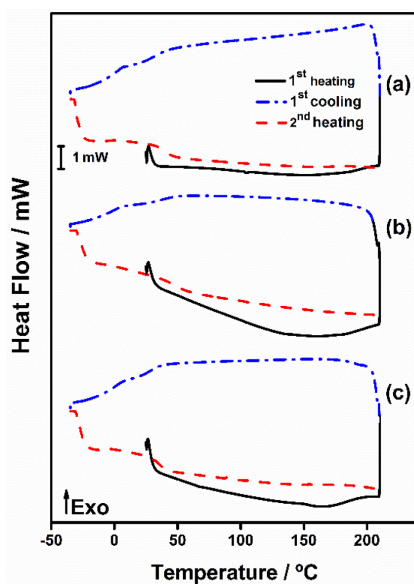


Figure 8. DSC curves of polymers a) PPF1, b) PPF2, and c) PPF3

temperature (T_{onset}) did not vary more than 11 °C (Table S3), it was possible to establish an order: PPF3 < PPF1 < PPF2.

3.7. SEM

Figure 9 exhibits the SEM images of obtained polymers. All samples exhibit an irregular surface, but each one have unique irregularities. The presence of porous could be related to the evaporation of water in the PP throughout the polymer synthesis. This property makes these polymers interesting as adsorbents, as investigated in a previous paper using macadamia vegetable oil as the precursor.²⁸

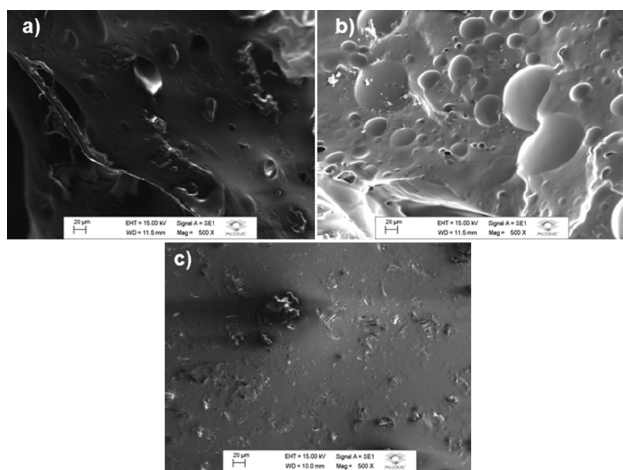


Figure 9. SEM images of a) PPF1, b) PPF2, and c) PPF3

4. Conclusions

Using a pre-polymer system and passion fruit vegetable oils produced by different extraction methods, renewable polymeric materials without using catalysts were obtained.

Furthermore, the vegetable oils presented a similar IV (around 123 g I₂ per gram of sample), thus considered semi-drying oils. The MIR analysis showed that the polymerization reaction occurred by consumption of the double bond of alkenes. In ¹H-NMR spectra of vegetable oils, all samples presented linoleic chains as the major polyunsaturated chains. In addition, TG/DTG-DTA curves of vegetable oils indicated that all samples, except for the PFVO3, were stable up to 270.0 °C. The lower thermal stability of PFVO3 could be associated with volatile molecules evaporation/degradation. Although the polymeric materials had less thermal stability due to the presence of water (on the surface or in cages), their thermal degradation profile was not considerably affected. The DSC curves of polymers also exhibited similar T_g values. Therefore, based on the previous results, the changes in the extraction procedures interfered with the physical chemical properties of the different passion fruit vegetable oils, which agrees with other papers in the literature. However, for the polymeric materials synthesized in the present work, the extraction procedure interfered mainly with the color of the final polymer without significant changes in the other properties, including thermal stability, T_g values, spectroscopic data, and morphology.

Acknowledgments

The authors thank CAPES (grants 024/2012 and 011/2009 Pro-equipment), FAPESP (grants: 2021/02152–9; 2021/14879–0; 2022/03489–0), and CNPq (grants 150233/2022–1 and 303247/2021–5) for financial support.

Conflict of Interest

The authors declare no conflict of interest.

References

- Geyer, R.; Jambeck, J. R.; Law, K. L.; Production, use, and fate of all plastics ever made. *Science Advances* **2017**, *3*, e1700782. [Crossref]
- Hong, M.; Chen, E. Y. X.; Future Directions for Sustainable Polymers. *Trends in Chemistry* **2019**, *1*, 148. [Crossref]
- Kaikade, D. S.; Sabnis, A. S.; Polyurethane foams from vegetable oil-based polyols: a review. *Polymer Bulletin* **2022**, *80*, 2239. [Crossref]
- Gong, L.; Passari, A. K.; Yin, C.; Kumar Thakur, V.; Newbold, J.; Clark, W.; Jiang, Y.; Kumar, S.; Gupta, V. K.; Sustainable utilization of fruit and vegetable waste bioresources for bioplastics production. *Critical Reviews in Biotechnology* **2024**, *44*, 233. [Crossref]
- Alarcon, R. T.; Gaglieri, C.; Lamb, K. J.; North, M.; Bannach, G.; Spectroscopic characterization and thermal behavior of baru nut

- and macaw palm vegetable oils and their epoxidized derivatives. *Industrial Crops and Products* **2020**, *154*, 112585. [Crossref]
6. Gaglieri, C.; Alarcon, R. T.; de Moura, A.; Magri, R.; da Silva-Filho, L.; Bannach, G.; Green and Efficient Modification of Grape Seed Oil to Synthesize Renewable Monomers. *Journal of the Brazilian Chemical Society* **2021**, *32*, 2120. [Crossref]
 7. Alarcon, R. T.; Gaglieri, C.; Souza, O. A.; Rinaldo, D.; Bannach, G.; Microwave-Assisted Syntheses of Vegetable Oil-Based Monomer: A Cleaner, Faster, and More Energy Efficient Route. *Journal of Polymers and the Environment* **2020**, *28*, 1265. [Crossref]
 8. Alarcon, R. T.; Lamb, K. J.; Bannach, G.; North, M.; Opportunities for the Use of Brazilian Biomass to Produce Renewable Chemicals and Materials. *ChemSusChem* **2020**, *14*, 169. [Crossref]
 9. Musik, M.; Bartkowiak, M.; Milchert, E.; Advanced Methods for Hydroxylation of Vegetable Oils, Unsaturated Fatty Acids and Their Alkyl Esters. *Coatings* **2021**, *12*, 13. [Crossref]
 10. Gaglieri, C.; Alarcon, R. T.; de Moura, A.; Bannach, G.; Vegetable oils as monomeric and polymeric materials: A graphical review. *Current Research in Green and Sustainable Chemistry* **2022**, *5*, 100343. [Crossref]
 11. Pereira, M. G.; Maciel, G. M.; Haminiuk, C. W. I.; Bach, F.; Hamerski, F.; de Paula Scheer, A.; Corazza, M. L.; Effect of Extraction Process on Composition, Antioxidant and Antibacterial Activity of Oil from Yellow Passion Fruit (*Passiflora edulis* Var. *Flavicarpa*) Seeds. *Waste and Biomass Valorization* **2018**, *10*, 2611. [Crossref]
 12. Nascimento, R. T.; Silva, H. de S.; Matos, J. M. E.; Santos, M. R. de M. C.; In vitro release and antioxidative potential of Pequi oil-based biopolymers (*Caryocar brasiliense* Cambess). *Journal of Polymer Research* **2019**, *26*, 1. [Crossref]
 13. Cheok, C. Y.; Adzahan, N. M.; Rahman, R. A.; Abedin, N. H. Z.; Hussain, N.; Sulaiman, R.; Chong, G. H.; Current trends of tropical fruit waste utilization. *Critical Reviews in Food Science and Nutrition* **2017**, *58*, 335. [Crossref] [PubMed]
 14. da Silva, A. C.; Jorge, N.; Bioactive compounds of oils extracted from fruits seeds obtained from agroindustrial waste. *European Journal of Lipid Science and Technology* **2016**, *119*, 1600024. [Crossref]
 15. Banerjee, J.; Singh, R.; Vijayaraghavan, R.; MacFarlane, D.; Patti, A. F.; Arora, A.; Bioactives from fruit processing wastes: Green approaches to valuable chemicals. *Food Chemistry* **2017**, *225*, 10. [Crossref] [PubMed]
 16. Mundo dos óleos. Available in: <https://www.mundodosoleos.com/> Access: March 31, 2023.
 17. de Oliveira, R. C.; de Barros, S. T. D.; Gimenes, M. L.; The extraction of passion fruit oil with green solvents. *Journal of Food Engineering* **2013**, *117*, 458. [Crossref]
 18. Byrne, F. P.; Jin, S.; Paggiola, G.; Petchey, T. H. M.; Clark, J. H.; Farmer, T. J.; Hunt, A. J.; McElroy, C. R.; Sherwood, J.; Tools and techniques for solvent selection: green solvent selection guides. *Sustainable Chemical Processes* **2016**, *4*, 1. [Crossref]
 19. Gaglieri, C.; de Moura, A.; Alarcon, R. T.; Magri, R.; Bannach, G.; Thermal behavior of some cyclic anhydrides: an important characterization for synthesis in the polymer field. *Journal of Thermal Analysis and Calorimetry* **2022**, *147*, 9095. [Crossref]
 20. American Society for Testing and Materials. ASTM D5554-15, Standard test method for determination of the iodine value of fats and oils. ASTM1: 2015.
 21. Guillén, M. D.; Ruiz, A.; Rapid simultaneous determination by proton NMR of unsaturation and composition of acyl groups in vegetable oils **2003**, *105*, 688. [Crossref]
 22. Silverstein, R. M.; Webster, F. X.; Kiemle, D. J.; Bryce, D. L.; *Spectrometric identification of organic compounds*, 8th ed., Wiley: New Jersey, 2005.
 23. Nahm, S.; Cheng, H.; Transition-state geometry and stereochemistry of the ene reaction between olefins and maleic anhydride. *Journal of Organic Chemistry* **1986**, *51*, 5093. [Crossref]
 24. Takam, P. N.; Djikeng, F. T.; Kuate, D.; Kengne, A. P. N.; Tsafack, H. D.; Makamwé, I.; Oben, J. E.; *Passiflora edulis* seed oil from west Cameroon: Chemical characterization and assessment of its hypolipidemic effect in high-fat diet-induced rats. *Food Science & Nutrition* **2019**, *7*, 3751. [Crossref] [PubMed]
 25. He, X.; Luan, F.; Yang, Y.; Wang, Z.; Zhao, Z.; Fang, J.; Wang, M.; Zuo, M.; Li, Y.; *Passiflora edulis*: An Insight Into Current Researches on Phytochemistry and Pharmacology. *Frontiers in Pharmacology* **2020**, *11*, 617. [Crossref] [PubMed]
 26. Santos, O. V.; Vieira, E. L. S.; Soares, S. D.; Conceição, L. R. V.; Nascimento, F. C. A.; Teixeira-Costa, B. E.; Utilization of agroindustrial residue from passion fruit (*Passiflora edulis*) seeds as a source of fatty acids and bioactive substances. *Food Science and Technology* **2020**, *41*, 1. [Crossref]
 27. Fulmer, G. R.; Miller, A. J. M.; Sherden, N. H.; Gottlieb, H. E.; Nudelman, A.; Stoltz, B. M.; Bercaw, J. E.; Goldberg, K. I.; NMR Chemical Shifts of Trace Impurities: Common Laboratory Solvents, Organics, and Gases in Deuterated Solvents Relevant to the Organometallic Chemist. *Organometallics* **2010**, *29*, 2176. [Crossref]
 28. Pires, O. A. B.; Alarcon, R. T.; Gaglieri, C.; da Silva-Filho, L. C.; Bannach, G.; Synthesis and characterization of a biopolymer of glycerol and macadamia oil. *Journal of Thermal Analysis and Calorimetry* **2018**, *137*, 161. [Crossref]